Journal of Applied Mechanics and Technical Physics, Vol. 42, No. 4, pp. 607–615, 2001

SUPERSONIC THREE-DIMENSIONAL FLOW AROUND TWO BODIES

N. N. Pilyugin[1] **and V. S. Khlebnikov**[2]

UDC 532.582.3.533.6.011.5

A supersonic three-dimensional flow around two bodies located one behind the other is experimentally studied. The flow structure between the bodies is analyzed. Zones of the maximum force loads on the surface of the rear body are determined.

Evolution of aviation and space technology raises interest to investigation of supersonic three-dimensional flows around two bodies located one behind the other. This is associated, on the one hand, with the problem of deceleration of flying vehicles (an axisymmetric body and a cruciform or gliding parachute), and, on the other hand, with separation of flying vehicles (an unmanned plane and an axisymmetric stage of the launcher).

In the present paper, we study experimentally a supersonic (Mach number M = 3) unsteady three-dimensional flow formed around two bodies. In the first test series, the front bodies had two, three, and four planes of symmetry (rectangular, triangular, and square end faces, respectively); the rear bodies were axisymmetric (circular end face). In the second test series, the front body was a cone or a sphere, and bodies with rectangular, triangular, and square end faces were used as a rear body.

The supersonic flow around a pair of bodies is complicated and diversified. This class of flows was mainly studied on axisymmetric pairs of isolated bodies. In a supersonic flow, depending on the distance between the bodies l_0, one of two flow patterns is formed [1–3]: a separated flow pattern with the flow separated from the front body and reattached to the rear body for $l_0 < l_0^*$ and a pattern with a base flow behind the front body and a bow shock wave ahead of the rear body for $l_0 \geqslant l_0^*$. Here l_0^* is the critical distance between the bodies at which one flow structure is transformed into the other. Flow reconstruction changes drastically the flow pattern around the bodies and, hence, significantly affects both the local and integral force and thermal characteristics of the rear body.

Many papers have been published recently, which deal with investigation of features of the above-mentioned axisymmetric flows [4–7]. In particular, the pressure and heat-flux distributions over the surface of a body located in a supersonic wake was obtained [8], the influence of the depth of the cavity and permeability of the rear body on the distribution of aerothermodynamic characteristics on the body surface was studied [9, 10], the aerodynamic drag of a pair of bodies connected by a cylindrical rod was measured [11], flow oscillations in the separation region between the bodies were determined [12], etc.

In the case of a three-dimensional flow around a pair of bodies, self-induced oscillations arise between the bodies, independent of the fact whether this flow is separated or has a shock wave ahead of the rear body. It is shown [13] that the flow near a sphere with a nonrotating spike with a plane tip at the end is three-dimensional (there are two planes of symmetry passing through the spike axis parallel to the major and minor bases of the tip). Two types of self-induced oscillations of the flow between the tip and the sphere are observed. The first type corresponds to oscillations in the case of flow separation from the tip or spike upstream of the sphere; the pressure in the reattachment region in one plane of symmetry of the pair of bodies differs significantly from the pressure in the other plane of symmetry, which makes the gas from the high-pressure region to flow to the low-pressure region and "splash" out from the separation region upstream of the sphere. The second type of oscillations is caused by the fact that the tip has different transverse dimensions in the planes of symmetry and, hence, critical distances at which flow reconstruction between the tip and the sphere in these planes occurs are also different: $l_1^* \neq l_2^*$. For this reason, the flow is unstable for $l_1^* \leqslant l_0 < l_2^*$: flow separation occurs alternatively from the tip and from the spike.

[1]Institute of Mechanics, Moscow State University, Moscow 119899. [2]Joukowski Central Aerohydrodynamic Institute, Zhukovskii 140180. Translated from Prikladnaya Mekhanika i Tekhnicheskaya Fizika, Vol. 42, No. 4, pp. 52–61, July–August, 2001. Original article submitted July 20, 2000.

0021-8944/01/4204-0607 $25.00

Self-induced oscillations exert a significant effect on the maximum heat-flux value in the reattachment region on the sphere.

The objective of the present work is to study the features of a supersonic three-dimensional flow around two bodies.

The front body in the experiments had a rectangular end face with sides $a = 17.5$ mm and $b = 35$ mm, regular triangular or square end faces with side length $a = 25$ mm, a cone with a base diameter $d^0 = 14$ mm and height $h^0 = 25$ mm, and spheres with diameters $d = 14$ and 18 mm. The front bodies were mounted on a thin side suspension with a rhombic profile, which was mounted at an angle of 60° to the incoming flow. The triangular face was attached to the sting at one of the apices. The height from this apex to the base of the triangle lies in the plane of symmetry of the sting. The rectangular face was attached to the sting in the middle of the minor base, and its plane of symmetry coincided with the plane of symmetry of the sting. The square face was attached to the sting in a similar manner. The cone and spheres were attached so that the planes of symmetry of the front body models coincided with the plane of symmetry of the sting.

The rear body had a circular face with diameter $D = 60$ mm, a rectangular face with sides $a_1 = 30$ mm and $b_1 = 60$ mm, a regular triangular face with side length $a_2 = 60$ mm, and a square face with side length $a_3 = 60$ mm. The rear body models were mounted on a cylindrical sting with a 30-mm external diameter, with pressure pipelines passing inside the sting. Places where pressure taps were located on the models are described below in discussing the results. In the course of experiments, the rear body could move along the flow with a prescribed step. The centers of the front and rear bodies were located on the same axis.

Since the flow between two bodies was unsteady, as was noted above, the readings of the group registering manometer had some fluctuations at the initial time of pressure measurement on the rear body. However, in a few seconds, the pressure in the measurement pipeline became steady (damped), after which the pressure was recorded. The measured value is the integral characteristic of this unsteady process.

The tests were performed in a supersonic wind tunnel with an axisymmetric test section and flow heating at M = 3, stagnation temperature $T_0 = (393 \pm 3)$ K, and stagnation pressure $P_0 = (49 \pm 0.1)$ N/cm^2. The Reynolds number based on the free-stream parameters and characteristic transverse size of the rear body varied within $10^6 \leqslant \mathrm{Re}_D \leqslant 1.4 \cdot 10^6$.

To obtain more detailed information on the flow between the bodies, the flow structure was visualized using a shadowgraph and laser sheet. In addition, the distribution of the limiting streamlines on the surface of the rear body was obtained.

We consider the case of the flow around a circular face located at different distances in the wake behind rectangular, square, and triangular faces. The pressure taps on the circular face were located in two directions: in the diameter plane, which coincided with the plane of the sting of the front body, and along the circle of radius $r_0 = 24$ mm.

Figures 1 and 2 show the pressure P on a circular face in the diameter plane as a function of the coordinate r (Fig. 1) and along the circle as a function of the coordinate φ (Fig. 2) in wakes behind rectangular, square, and triangular faces for different distances l between the bodies. Here P is the ratio of the pressure at a certain point on the end face p to the stagnation pressure behind the normal shock in the free stream p_0', r is the ratio of the coordinate of the point r_1 counted from the face center in the radial direction to the face radius R (the coordinate is positive in the direction to the sting of the front body and negative in the opposite direction), φ is the central angle on the face counted along the circle from the plane of the sting of the front body, and l is the ratio of the distance between the bodies (l_0) and the diameter (d_1) of the circle described around the front body.

In contrast to the axisymmetric case, the three-dimensional flow between two bodies is unsteady (self-induced oscillations are observed), as well as in the case of the flow around a sphere with a spike that has a plane tip at the end. Reconstruction of a separated flow into a flow with a bow shock wave ahead of the rear body depends on the ratio of the front body dimensions to the rear body diameter and the distance between them.

It should be noted that the character of the flow between the bodies and the pressure distribution on the rear face may be significantly affected by the sting of the front body.

In a separated flow between two bodies for all the above types of the front body, the pressure distribution in the diameter plane of the rear face has the same character as in the case of the flow around an axisymmetric pair of bodies [2]. In this case, the sting of the front body has a significant effect on the pressure behind it for $r > 0$ (curves 1 in Fig. 1). After reconstruction of the separated flow between the bodies, at the point where the influence of the sting of the front body is weak, the pressure on the rear face increases severalfold (curves 2 and 3

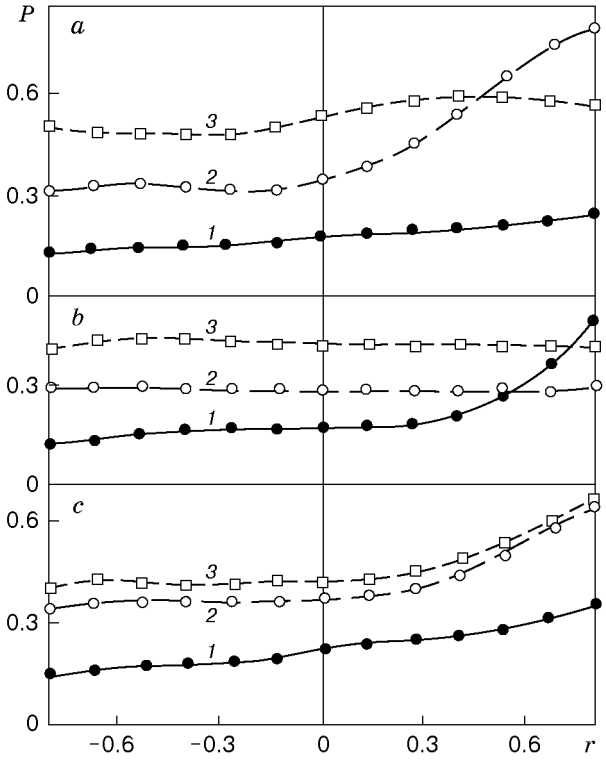

Fig. 1

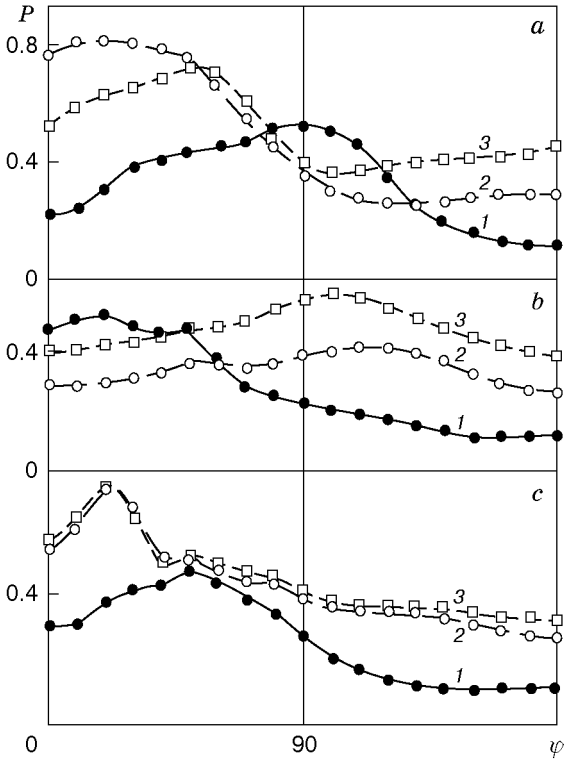

Fig. 2

Fig. 1. Pressure distribution on a circular face in the diameter plane, in the wake behind rectangular (a), square (b), and regular triangular (c) faces: curve 1 refers to the separated flow [$l = 3.4$ (a) and 3.6 (b and c)]; curve 2 refers to the flow with a shock wave upstream of the rear face for $l = 3.8$ (a) and $l = 4.8$ (b and c) and curve 3 refes to the flow with a shock wave upstream of the rear face for $l = 5.7$ (a), $l = 8.0$ (b), and $l = 7.2$ (c).

Fig. 2. Circumferential pressure distribution on a circular face in the wake behind rectangular (a), square (b), and regular triangular (c) faces (notation the same as in Fig. 1).

in Fig. 1). The effect of the sting of the front body on the pressure in the diameter plane behind it ($r > 0$) behind a triangular face remains almost unchanged (curves 2 and 3 in Fig. 1c). Behind a rectangular face, this influence is significant only immediately after the reconstruction of the separated flow (curve 2 in Fig. 1a) and is rapidly attenuated with increasing distance between the front face and the rear body (curve 3 in Fig. 1a). This effect is almost absent behind a square face (curves 2 and 3 in Fig. 1b).

An analysis of pressure distribution along the face edge (Fig. 2) shows that the character of the dependence $P(\varphi)$ changes significantly with changing distance l. For instance, the maximum pressure behind a rectangular face for $l = 3.4 < l^*$ was observed for $\varphi = 90°$, and the minimum pressure was obtained for $\varphi = 180°$ (curve 1 in Fig. 2a). After the reconstruction of the separated flow at $l = 5.7 > l^*$, the minimum pressure was observed for $\varphi = 100°$, and the maximum pressure was obtained for $\varphi = 180°$ (curve 3 in Fig. 2a). The difference in pressure values along the edge of a circular face leads to gas overflow from the high-pressure region to the low-pressure region, which results in oscillations of the separated flow and the bow shock wave ahead of the rear face after flow reconstruction.

We consider the flow features between axisymmetric bodies (cones or spheres) and rectangular, square, or triangular faces in a supersonic flow regime.

A rectangular (square) end face was located in the wake so that the plane of symmetry passing through the middle of the smaller side (one of the sides) and the center of the face coincided with the plane of symmetry of the sting of the front body. A regular triangular face was placed in the wake so that one of the triangle apices was located behind the sting of the front body, and the height from this apex to the opposite side was in the plane of symmetry of the sting.

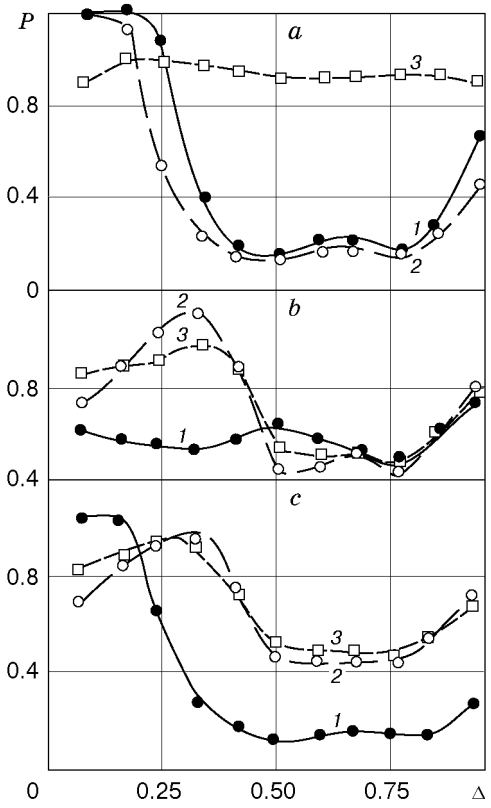

Fig. 3

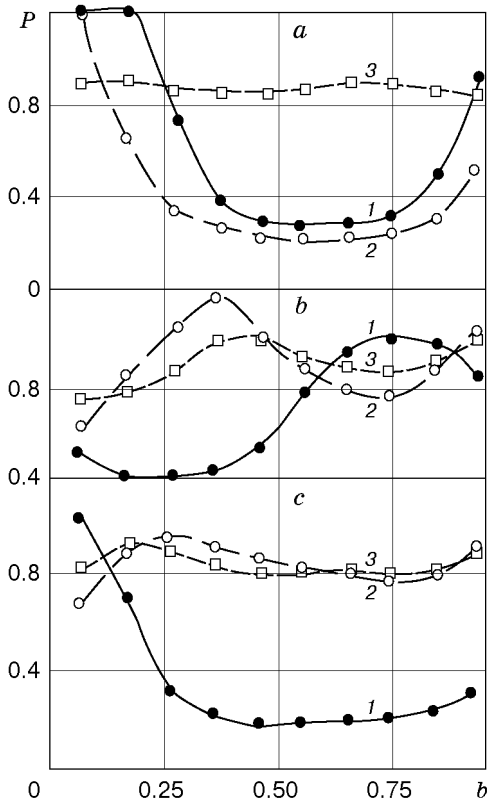

Fig. 4

Fig. 3. Pressure distribution on a rectangular face along its diagonal in the wake behind a cone (a) and spheres with $d = 14$ (b) and 18 mm (c): (a) $l = 5.0$ (1), $l = 7.1 < l^*$ (2), and $l = 9.3 > l^*$ (3); (b) $l = 5.1 < l^*$ (1), $l = 7.3$ (2), and $l = 9.4 > l^*$ (3); (c) $l = 3.9 < l^*$ (1), $l = 5.6$ (2), and $l = 7.2 > l^*$ (3).

Fig. 4. Pressure distribution on a rectangular face along its side b_1 in the wake behind a cone (a) and spheres with $d = 14$ (b) and 18 mm (c) (notation the same as in Fig. 3).

On face surfaces, we determined directions along which the pressure was measured. For a rectangular face, the pressure taps were located along its diagonal and the side b_1. The origin for both directions of pressure measurement on the face was located near their intersection point behind the sting of the front body (in the first case, in the rectangle apex, and in the second case, on the side a_1). The pressure taps on the square face were located in a similar way; and the origin for each direction of pressure measurement was chosen.

On the triangular face, the pressure taps were located in two directions: along the height of the triangle in the plane of the sting of the front body and in the perpendicular direction parallel to the side a_2. The origin on the face surface for pressure measurement along these lines was chosen at the point of their intersection. The characteristics of flows between axisymmetric bodies and rectangular, square, and triangular faces are mainly analyzed by pressure distributions obtained for different front bodies and distances between the bodies. The results of pressure measurement were supplemented by flow visualization.

Figures 3 and 4 show the pressure distributions on a rectangular face along its diagonal (Fig. 3) and side b_1 (Fig. 4) in the wake behind a cone and spheres. Here Δ is the ratio of the coordinate along the rectangle diagonal Δ_0 to its length Δ_1, b is the ratio of the coordinate along the rectangle side b_0 to its length b_1, $l = l_0/d$, and $l^* = l_0^*/d$.

The results of flow visualization are shown in Fig. 5. An analysis of the photographs shows that either a separated flow or a flow with a bow shock wave upstream of the face (depending on the distance between the bodies) is formed, as in the case of an axisymmetric flow around a pair of models [3]. However, there are some special features in our case. For instance, a shock wave is observed in the separated flow in the region of flow reattachment in the vicinity of the face part protruding into the undisturbed flow (frames 1 in Fig. 5a and b). This is also confirmed by the distribution of the limiting streamlines shown in Fig. 6a: there are divergence lines near

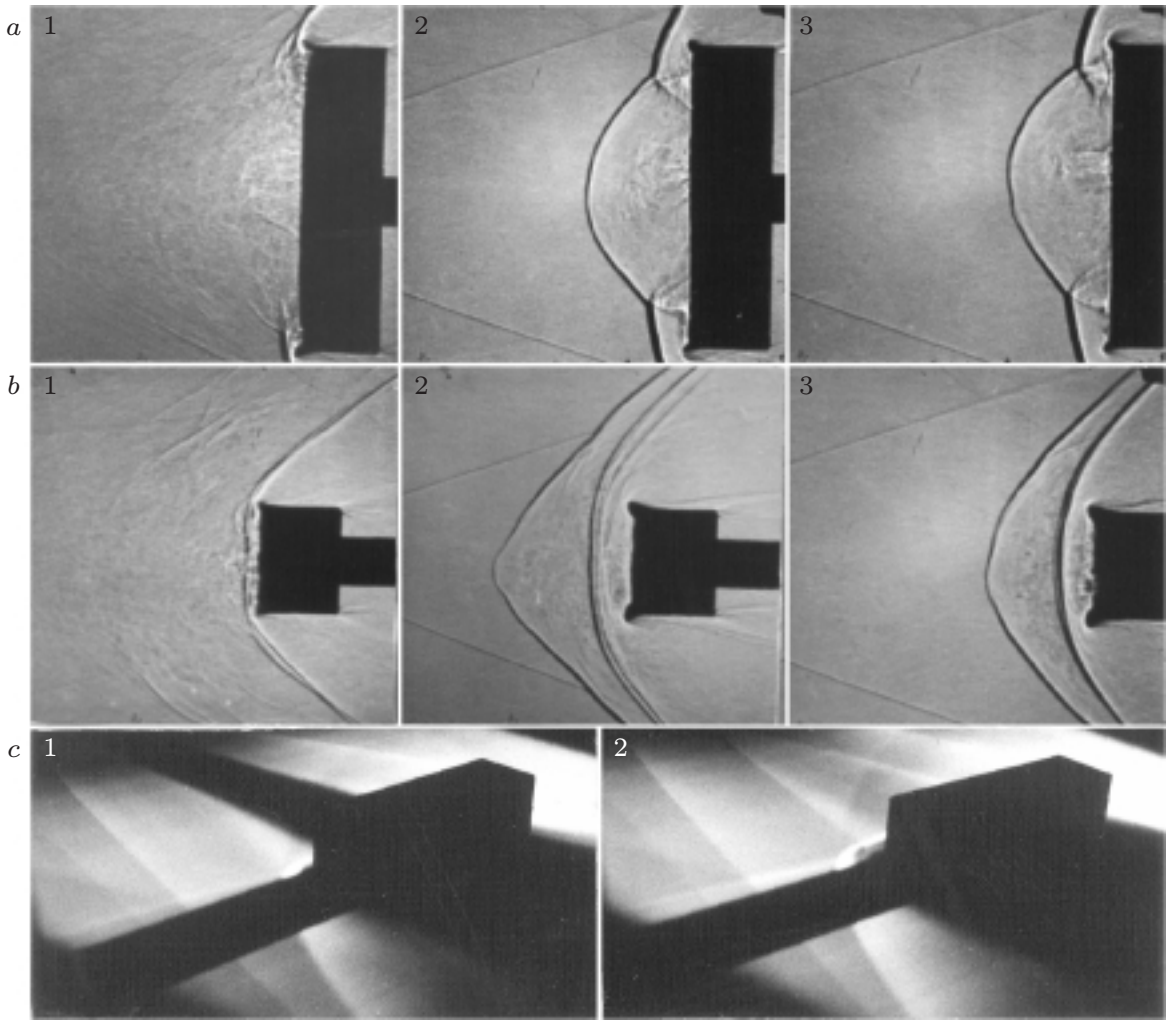

Fig. 5. Visualization of the flow structure around a rectangular face in the wake behind a sphere ($d = 18$ mm): (a, b) schlieren pictures in two mutually perpendicular planes (parallel to the major and minor bases of the rectangular face, respectively [$l < l^*$ (1) and $l > l^*$ (2 and 3)]; (c) laser sheet picture [$l < l^*$ (1) and $l > l^*$ (2)].

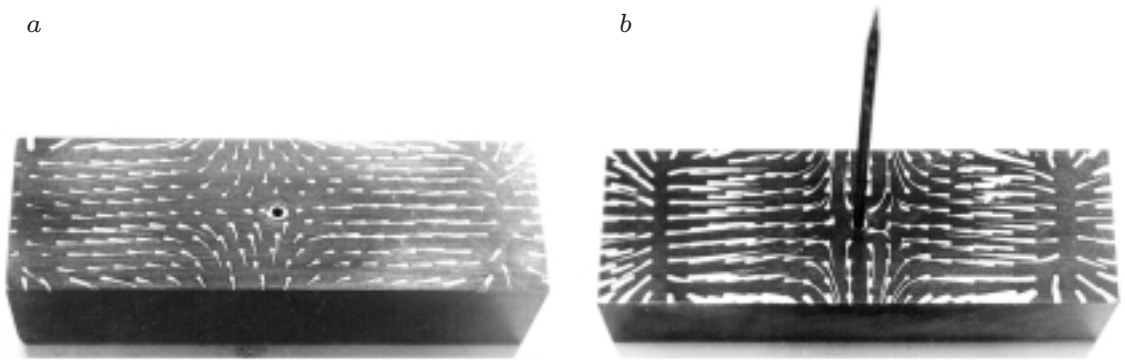

Fig. 6. Distribution of the limiting streamlines on a rectangular face: in the separated flow (a) and in the flow around a face with a spike (b).

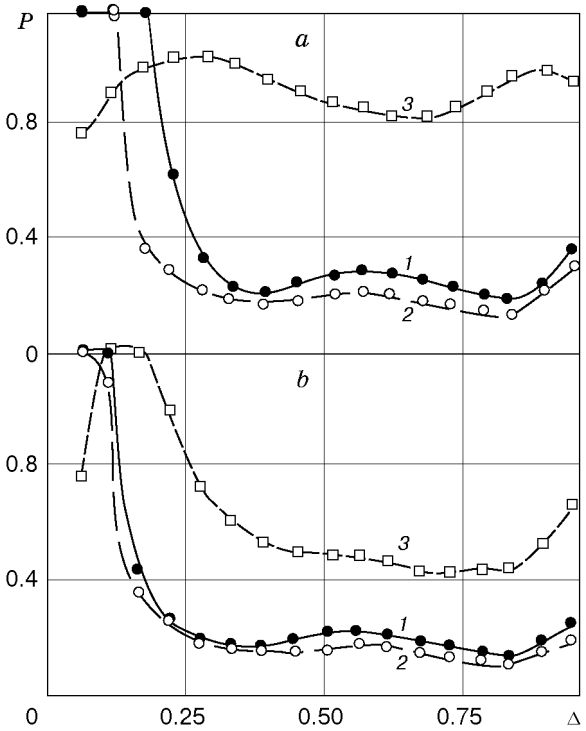

Fig. 7

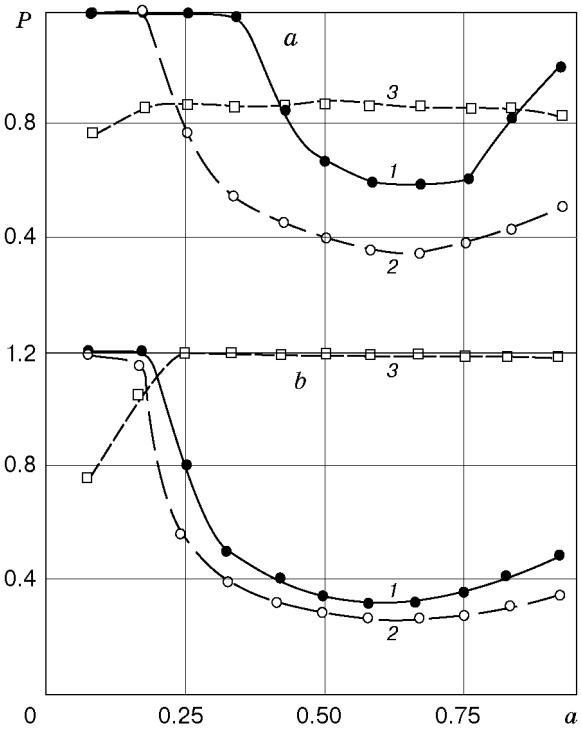

Fig. 8

Fig. 7. Pressure distribution on a square face along its diagonal in the wake behind a cone (a) and a sphere with $d = 18$ mm (b): (a) $l = 5.7$ (1), $l = 7.9 < l^*$ (2), and $l = 10.0 > l^*$ (3); (b) $l = 4.8$ (1), $l = 8.4 < l^*$ (2), and $l = 9.5 > l^*$ (3).

Fig. 8. Pressure distribution on a square face along its side a_3 in the wake behind a cone (a) and a sphere with $d = 18$ mm (b) (notations the same as in Fig. 7).

the face ends protruding into the undisturbed flow. The flow along the rear body moves toward the face center and "splashes" out on both sides in the vicinity of the minor axis of symmetry of the face. For comparison, Fig. 6b shows the distribution of the limiting streamlines in a separated flow around a face with a spike. The character of distributions of the limiting streamlines is similar to that described above.

An analysis of test results shows that the flow between the bodies is unsteady. This is evidenced by frame records of the flow around the bodies and pressure fluctuations on the rectangular face.

It follows from the analysis of pressure distribution on the face in a separated flow (curves 1 in Fig. 3 and curve 2 in Fig. 3a) that the pressure increases when approaching the face edge ($\Delta = 0.93$), where a shock wave is observed.

After reconstruction, the three-dimensional flow near the rear body differs from a similar axisymmetric flow [2]. In this case, the bow shock wave ahead of the face is split into a pair of shocks. Near the wake axis, because of the valley in the total pressure profile, the bow shock wave ahead of the rear body is extended toward the front body and becomes plane near the face parts protruding from the wake (frames 2 and 3 in Fig. 5a and b). As a result, the shock-wave configuration may change, depending on the angle of intersection and shock-wave strength in the region of interaction. Extreme values of the thermal and force loads on the face should be expected in this region.

Laser sheet visualization of both flow patterns between the sphere and rectangular face is shown in Fig. 5c.

An analysis of pressure distribution on the rectangular face after reconstruction of the separated flow between the bodies shows that there is no pressure peak near the face edge if the front body (cone) has low drag (curve 3 in Fig. 3a); the pressure near the face edge ($\Delta = 0.93$) increases significantly if the front body (sphere) has high drag (curves 2 and 3 in Fig. 3b and c). The pressure at the center of the face ($\Delta = 0.5$) is greater for lower losses in the bow shock wave ahead of the front body (curves 3 in Fig. 3a and c).

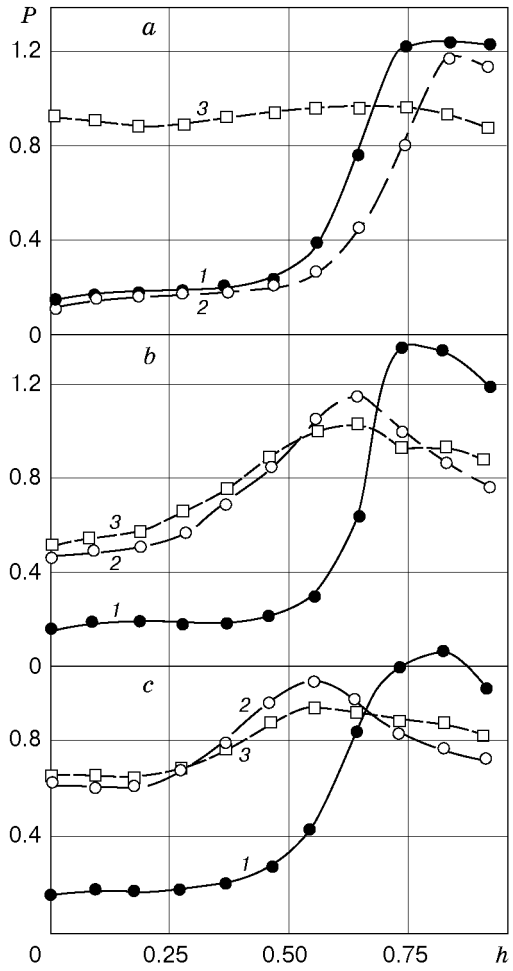

Fig. 9

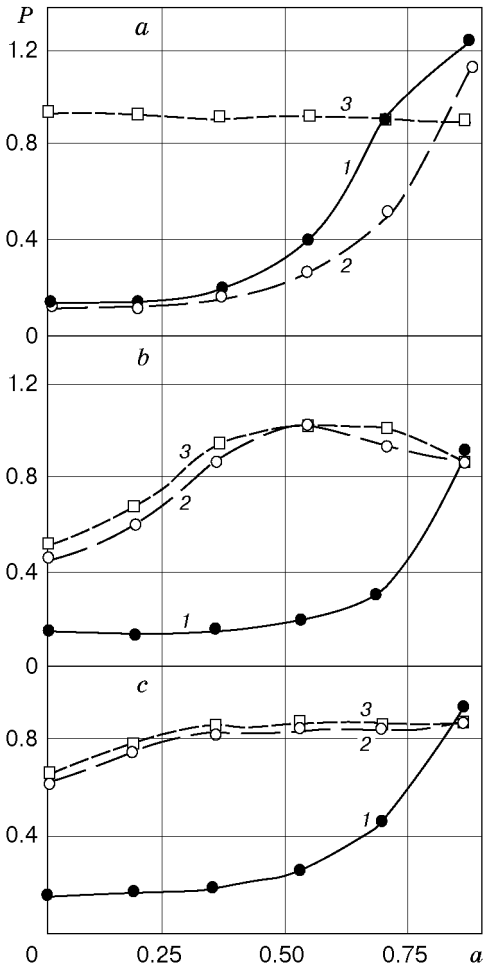

Fig. 10

Fig. 9. Pressure distribution on a regular triangular face along the height in the wake behind a cone (a) and spheres with $d = 14$ (b) and 18 mm (c): (a) $l = 5.0$ (1), $l = 7.1 < l^*$ (2), and $l = 9.3 > l^*$ (3); (b) $l = 5.2 < l^*$ (1), $l = 7.3$ (2), and $l = 9.4 > l^*$ (3); (c) $l = 3.9 < l^*$ (1), $l = 5.6$ (2), and $l = 7.2 > l^*$ (3).

Fig. 10. Pressure distribution on a regular triangular face along its side in the wake behind a cone (a) and spheres with $d = 14$ (b) and 18 mm (c) (notation the same as in Fig. 9).

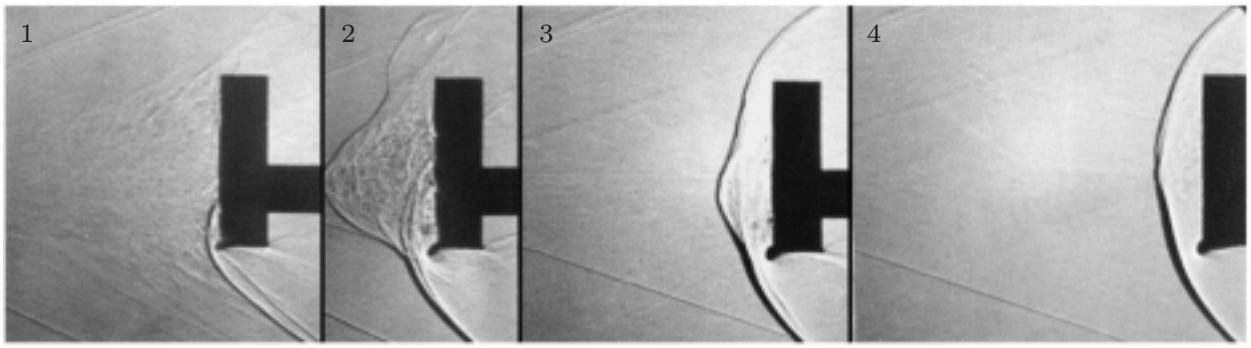

Fig. 11. Photographs of the flow pattern around a regular triangular face in the wake behind a cone: separated flow (frame 1) and flow with a bow shock wave at different distances from the cone (frames 2–4) for $l = 5.0 < l^*$ (2), $l = 10.1$ (3), and $l = 11.0 > l^*$ (4).

For all distances between the bodies, the pressure distribution along the side b_1 has the same character as the distribution along the diagonal (curves 1 and 3 in Figs. 3a and c and 4a and c).

Figures 7 and 8 show the pressure distributions on a rectangular face along its diagonal (Fig. 7) and the side a_3 (Fig. 8) in the wake behind a cone and a sphere. Here Δ is the ratio of the coordinate along the square diagonal Δ_0 to its length Δ_3 and a is the ratio of the coordinate along the square side a_0 to its length a_3.

It follows from the dependences in Figs. 7 and 8 that the results of pressure measurement on a rectangular face in the wake behind an axisymmetric body are also valid for a square face. It should be noted that, for a sphere–square face pair, the pressure along the side a_3 after reconstruction of the separated flow between the bodies is almost constant and approximately 20% greater than the stagnation pressure behind the normal shock in the undisturbed flow. This is explained by the fact that the flow arriving at the side a was decelerated in several oblique shock waves, and the losses in these shocks are lower than in the normal shock. Note also that the sting of the front body, for all distances between the bodies examined, has a significant effect on the value of pressure on rectangular faces for $\Delta < 0.4$ (Fig. 3) and $b < 0.4$ (Fig. 4) and square faces for $\Delta < 0.25$ (Fig. 7) and $a < 0.35$ (Fig. 8).

Figures 9 and 10 show the pressure distributions on a regular triangular face along the height h (Fig. 9) and the side a (Fig. 10) in the wake behind a cone and spheres. Here h is the ratio of the ordinate h_0 to the distance from the origin to the triangle apex h_{02} and a is the ratio of the abscissa a_0 to the length of its measurement range a_{02}.

Figure 11 shows the Schlieren pictures of the flow around a cone–triangular face pair for different distances between the bodies. As in the case of the flow around the cone (sphere)–rectangular (square) face, the flow is unsteady for all distances between the bodies examined.

In the flow around a cone (sphere)–triangular face pair at $l < l^*$, a separated flow is formed (frame 1 in Fig. 11). In this case, the pressure in the origin is severalfold smaller than the pressure at the triangle apex, for example, in the wake behind a cone — by a factor of 7 to 8 (curves 1 and 2 in Fig. 10a). The pressure at the triangle apex $P = 1.2$ is considerably greater than the stagnation pressure behind the shock wave in the undisturbed flow. The reason is, on the one hand, the presence of a shock wave upstream of the triangle apex protruding from the wake (frame 1 in Fig. 11) and, on the other hand, by the fact that the flow arriving at this shock was prior decelerated in oblique shock waves. Because of the pressure difference along the edge of the triangular face, gas overflow from the high-pressure region to the low-pressure region should be expected.

For $l > l^*$, the separated flow between the bodies is reconstructed (frames 2–4 in Fig. 11). Because of that, the pressure in the center of the face ($h = 0.3$) increases severalfold, depending on the drag of the front body. Thus, the pressure behind the cone increases by a factor of 4.5 (curves 2 and 3 in Fig. 9a) and by a factor of 3.5 behind a sphere ($d = 18$ mm) (curves 1 and 2 in Fig. 9c). In addition, the pressure along the face edge in the wake behind the cone is almost constant (curve 3 in Fig. 10a), which is confirmed by the shape of the shock wave ahead of the face (frame 4 in Fig. 11). In the wake behind a sphere, the pressure along the face edge changes significantly (curves 2 and 3 in Fig. 10b), which should lead to gas overflow along the latter.

As in the cases of the wake flow around rectangular and square faces, the sting of the front body has a significant effect on the pressure behind it on a triangular face (see Fig. 9) ($h > 0.65$).

Based on the above results, the special features of flows formed in the case of a supersonic three-dimensional flow around two bodies are analyzed.

This work was supported by the Federal Goal-Oriented Program “Integration” (Grant No. I(A-105-4)).

REFERENCES

1. A. F. Charwat, J. N. Roos, F. C. Dewey, and J. A. Hitz, “An investigation of separated flows. Part 1. The pressure field,” *J. Aerospace Sci.*, **28**, No. 6, 457–470 (1961).
2. V. S. Khlebnikov, “Supersonic axisymmetric gas flow around a pair of bodies,” *Uch. Zap. TsAGI*, **9**, No. 6, 108–114 (1978).
3. V. S. Khlebnikov, “Supersonic flow pattern around a pair of bodies and reconstruction of the flow between them,” *Izv. Ross. Akad. Nauk, Mekh. Zhidk. Gaza*, No. 1, 158–165 (1994).
4. P. Chang, *Separation of Flow*, Vol. 3, Pergamon Press, Oxford (1970).
5. V. N. Kudryavtsev, A. Ya. Cherkez, and V. A. Shilov, “Supersonic flow around two separating bodies,” *Izv. Akad. Nauk SSSR, Mekh. Zhidk. Gaza*, No. 2, 91–99 (1969).

6. Yu. P. Golovachev and N. V. Leont'eva, "Numerical study of the flow around a blunted body in a supersonic wake," Preprint No. 918, Yoffe Physicotechnical Institute, Leningrad (1984).
7. I. A. Belov, I. M. Dement'ev, and S. A. Isaev, "Modeling of a supersonic flow around bodies of revolution with a front separation region," Preprint No. 1033, Yoffe Physicotechnical Institute, Leningrad (1986).
8. I. G. Eremeitsev, N. N. Pilyugin, V. S. Khlebnikov, and S. A. Yunitskii, *Investigation of Aerodynamic Characteristics and Heat Transfer of Bodies in Nonuniform Supersonic Gas Flows* [in Russian], Izd. Mosk. Univ., Moscow (1988).
9. V. S. Khlebnikov, "Effect of the depth of the cavity on pressure and heat-flux distributions over the bottom of a "glass" located in a supersonic wake behind the body," *Tr. TsAGI*, No. 1763, 22–38 (1976).
10. V. S. Khlebnikov, "Axisymmetric supersonic wake flow around a ducted body," *Tr. TsAGI*, No. 1987, 13–20 (1987).
11. V. S. Khlebnikov, "Drag of a pair of bodies in transonic and supersonic flows," *Izv. Akad. Nauk SSSR, Mekh. Zhidk. Gaza*, No. 3, 152–156 (1990).
12. V. I. Zapryagaev, "Pulsations in the separation zone of a free cavern at a supersonic stream velocity," *Prikl. Mekh. Tekh. Fiz.*, **26**, No. 6, 50–58 (1985).
13. V. S. Khlebnikov, "Experimental study of a supersonic three-dimensional separated flow between a plane tip and a sphere," *Izv. Akad. Nauk SSSR, Mekh. Zhidk. Gaza*, No. 5, 166–170 (1987).